A Synthetic Protocell-Based Heparin Scavenger

Please check the document version of this publication:

• A submitted manuscript is the version of the article upon submission and before peer-review. There can be important differences between the submitted version and the official published version of record. People interested in the research are advised to contact the author for the final version of the publication, or visit the DOI to the publisher's website.
• The final author version and the galley proof are versions of the publication after peer review.
• The final published version features the final layout of the paper including the volume, issue and page numbers.

[Link to publication](#)

A Synthetic Protocell-Based Heparin Scavenger

Qing Liu, Shuo Yang, Iris Seitz, Anna-Maria Makri Pistikou, Tom F. A. de Greef,* and Mauri A. Kostiainen*

Heparin is a commonly applied blood anticoagulant agent in clinical use. After treatment, excess heparin needs to be removed to circumvent side effects and recover the blood-clotting cascade. Most existing heparin antidotes rely on direct heparin binding and complexation, yet selective compartmentalization and sequestration of heparin would be beneficial for safety and efficiency. However, such systems have remained elusive. Herein, a semipermeable protein-based microcompartment (proteinosome) is loaded with a highly positively charged chitosan derivative, which can induce electrostatics-driven internalization of anionic guest molecules inside the compartment. Chitosan-loaded proteinosomes are subsequently employed to capture heparin, and an excellent heparin-scavenging performance is demonstrated under physiologically relevant conditions. Both the highly positive scavenger and the polyelectrolyte complex are confined and shielded by the protein compartment in a time-dependent manner. Moreover, selective heparin-scavenging behavior over serum albumin is realized through adjusting the localized scavenger or surrounding salt concentrations at application-relevant circumstances. In vitro studies reveal that the cytotoxicity of the cationic scavenger and the produced polyelectrolyte complex is reduced by protocell shielding. Therefore, the proteinosome-based systems may present a novel polyelectrolyte-scavenging method for biomedical applications.

1. Introduction

Selective compartmentalization is a fundamental biological function responsible for reaction cascading, substrate sorting, and removal of toxic substances. In eukaryotes, this is realized through specific uptake pathways that are mediated by the signals recognized on substrate targets.[1] For instance, essential nutrients are internalized via clathrin-mediated endocytosis while caveolae-mediated endocytosis is mainly responsible for the transport of vesicular cargos.[2] In many viruses, the genetic material is recognized and packaged during the protein capsid formation,[3] and others may uptake noncognate cargo after the formation of capsids.[4] In the latter case, openings in the protein shell are required for the cargo trafficking, and selected substrates can be targeted through regulating the pore properties.[5] Alternative to the pore engineering, the interior surface of capsids can also be engineered to control the substrate influx via electrostatic or hydrophobic interactions.[6]

Continuous efforts have been devoted to elucidating the naturally occurring internalization in an attempt to understand this fundamental biological process and eventually achieve biomedical goals.[7] Artificial protocells prepared from polymers (polymersomes),[8] inorganic nanoparticles (colloidosomes),[9] and protein–polymer conjugates (proteinosomes)[10] have recently emerged as a robust study model owing to their semipermeable membrane structures. Incidentally, these artificial protocells exhibit cell-mimicking behavior, i.e., spatial positioning,[11] extracellular signal responsiveness[12] and predatory behavior.[9a] In spite of their potential, the biomedical applications of such protocells have been scarcely exploited.[13]

Here, we investigated the potential of artificial proteinosomes for heparin scavenging.[10] Heparin is a widely used anticoagulant agent in many clinical applications.[14] However,

Q. Liu
Wenzhou Institute
University of Chinese Academy of Sciences (WIUCAS)
Wenzhou, Zhejiang 325001, China

Q. Liu, I. Seitz, M. A. Kostiainen
Biohybrid Materials
Department of Bioproducts and Biosystems
Aalto University
Espoo 02150, Finland
E-mail: mauri.kostiainen@aalto.fi

The ORCID identification number(s) for the author(s) of this article can be found under https://doi.org/10.1002/smll.202201790.

S. Yang, A.-M. M. Pistikou, T. F. A. de Greef
Laboratory of Chemical Biology
Department of Biomedical Engineering
Computational Biology Group
Department of Biomedical Engineering and
Institute for Complex Molecular Systems
Eindhoven University of Technology
Eindhoven, MB 5600, The Netherlands
E-mail: t.f.a.d.greef@tue.nl

T. F. A. de Greef
Institute for Molecules and Materials
Radboud University
Nijmegen, MB 6525, The Netherlands

T. F. A. de Greef
Center for Living Technologies
Alliance TU/e, WUR, UU, UMC Utrecht
Utrecht, CB 3584, The Netherlands

fast and complete removal of heparin is needed when the blood-clotting cascade needs to be restored. More importantly, excessive heparin use can induce severe side effects, such as low blood platelet levels and heparin-induced thrombocytopenia.[15] Protamine sulfate (PS) has been serving as the only clinically approved antidote for heparin for the past 80 years.[14] However, adverse effects provoked by PS and PS-heparin complex rise general concern.[16] Therefore, various cationic alternatives such as (bio)polymers,[17] self-assembled systems,[18] and engineered proteins[19] have been utilized as alternative heparin-scavengers, which take advantage of the highly anionic nature of heparin and rely on electrostatic binding. Among the proposed approaches, selective sequestration of heparin into an environment-inert compartment attracts particular interest since cationic heparin binders and the produced polyelectrolyte complexes raise general safety issues.[16,19b]

In this work, we prepared semipermeable and biocompatible proteinosomes loaded with a highly positively charged chitosan derivative. Its heparin-scavenging ability was found to be comparable to PS under application-relevant conditions (PBS: 10 M phosphate buffer, 150 M NaCl, pH 7.5), and selective heparin-scavenging performance was achieved through adjusting the local scavenger or the surrounding salt concentrations. Therefore, such a compartmentalized system presents a general method for the selective removal of polyelectrolytes in vitro and in vivo.

2. Results and Discussion

To encapsulate chitosan, we employed proteinosomes, hollow microcapsules based on cross-linked bovine serum albumin-poly(N-isopropylacrylamide) (BSA-PNIPA) conjugates.[10,20] Depending on the cross-link density, the semipermeable membrane has a molecular weight cutoff ranging from 40 to 80 kDa.[20] Therefore, chitosan with a molecular weight of 310–375 kDa was used to ensure an efficient confinement. The biomass-derived chitosan was cationized with glycidyltrimethylammonium chloride, yielding the highly positively charged derivative, N-[(2-hydroxy-3-trimethylammonium)propyl]chitosan (HTCC).[21] Unfractionated heparin (M_w: 6–30 kDa, mean 17–19 kDa) was utilized, and human serum albumin (HSA, 66.5 kDa) was used as a competitive molecule to mimic the physiological environment because it is the most abundant protein in blood plasma.[22] To visualize the internalization of guest molecules and the morphology transformation within proteinosomes, HTCC, heparin, and HSA were labeled with orthogonal fluorescent dyes (green fluorescein (FITC) for HTCC, yellow Rhodamine B for heparin, and red Cy5 for HSA). Nuclear magnetic resonance spectra and fluorescence spectroscopy verified the successful production of HTCC and the fluorescently labeled materials (Figures S1–S3, Supporting Information).

In order to encapsulate HTTC, an aqueous solution containing FITC-labeled HTCC and BSA–PNIPA conjugates was mixed with oil, resulting in a Pickering emulsion where the conjugates self-assembled at the interface while the hydrophilic HTCC remained in the aqueous interior of the emulsion droplets. The BSA on the interface was subsequently crosslinked with poly(ethylene glycol)-bis(N-succinimidyl succinate),

producing the desired HTCC-loaded proteinosomes after being transferred into water by dialysis, as illustrated in **Figure 1**a. Proteinosomes with two local HTCC concentrations were prepared: 0.23 mg mL^{-1} (PH1) and 0.77 mg mL^{-1} (PH2). As can be seen in Figure 1b,c and Figure S4 (Supporting Information), under the bright field of confocal fluorescence microscopy (CFM) proteinosomes with or without loading showed a typical transparent lumen with a spherical structure.[10] When HTCC was encapsulated, proteinosomes exhibited higher optical contrast than the empty ones. A green fluorescence emission dispersed throughout the cavity was observed, demonstrating the successful encapsulation of HTCC. Proteinosomes had diameters of 20–50 μm, and increasing the local HTCC concentration slightly enlarged the proteinosome size (Figure 1d). Zeta potential measurements results unveiled that the fluorescent labeling had an insignificant impact on the zeta potential: plain HTCC, heparin and HSA had values close to zero both before and after labeling (Table S1, Supporting Information). The confinement of HTCC into proteinosomes significantly enhanced the measured cationic nature and increasing HTCC concentration augmented the zeta potential: while the value was increased to 16.7 ± 1.3 mV for PH1, it was further increased to 26.7 ± 1.6 mV for PH2, which could be attributed to the increased local concentration of HTCC.

The heparin-scavenging ability of free HTCC was first evaluated with the methylene blue (MB)–displacement assay in phosphate buffer (PB: 10 M, 5 M NaCl, pH 7.5).[19] As shown in Figure 1e and Figure S5 (Supporting Information), bulk HTCC showed an excellent heparin-scavenging performance, which was similar to the clinical PS heparin antidote. A saturation point was reached approximately at a mass ratio of 2 (scavenger/heparin) for both scavengers, demonstrating the excellent heparin-scavenging ability of HTCC.[23] The heparin-binding performance in PB was also demonstrated by dynamic light scattering (DLS) measurements (Figure S6, Supporting Information). Furthermore, an efficient heparin neutralization performance under physiological-relevant conditions (PBS) was also revealed by an application-specific anti-Xa assay and DLS measurements (Figure 1e and Figures S7 and S8, Supporting Information).

In contrast to the instant heparin-capture by HTCC under batch conditions, heparin was gradually absorbed by HTCC-loaded proteinosomes, as demonstrated by the MB displacement assay (Figure S9, Supporting Information). This indicates that the electrostatically driven interaction between HTCC and heparin was partially restricted, but not blocked, by the protein membrane. Complete heparin-scavenging was achieved in 2 h, and for both PH1 and PH2 a mass ratio of about 2.5 (HTCC/heparin) at the saturation point was observed in PB, which verified the heparin-scavenging ability of HTCC within proteinosomes. The morphology of proteinosomes after the assay was directly visualized under an optical microscope (insets in Figure S9, Supporting Information). Compared to neat HTCC-containing proteinosomes shown in Figure 1c and Figure S4 (Supporting Information), proteinosomes after heparin internalization exhibited high optical contrast, demonstrating the formation of the polyelectrolyte complex in the cavity.[11,24] The encapsulation of HTCC and the internalization of heparin into a population of protocells were further confirmed by statistical measurements using flow cytometry (Figure S10, Supporting
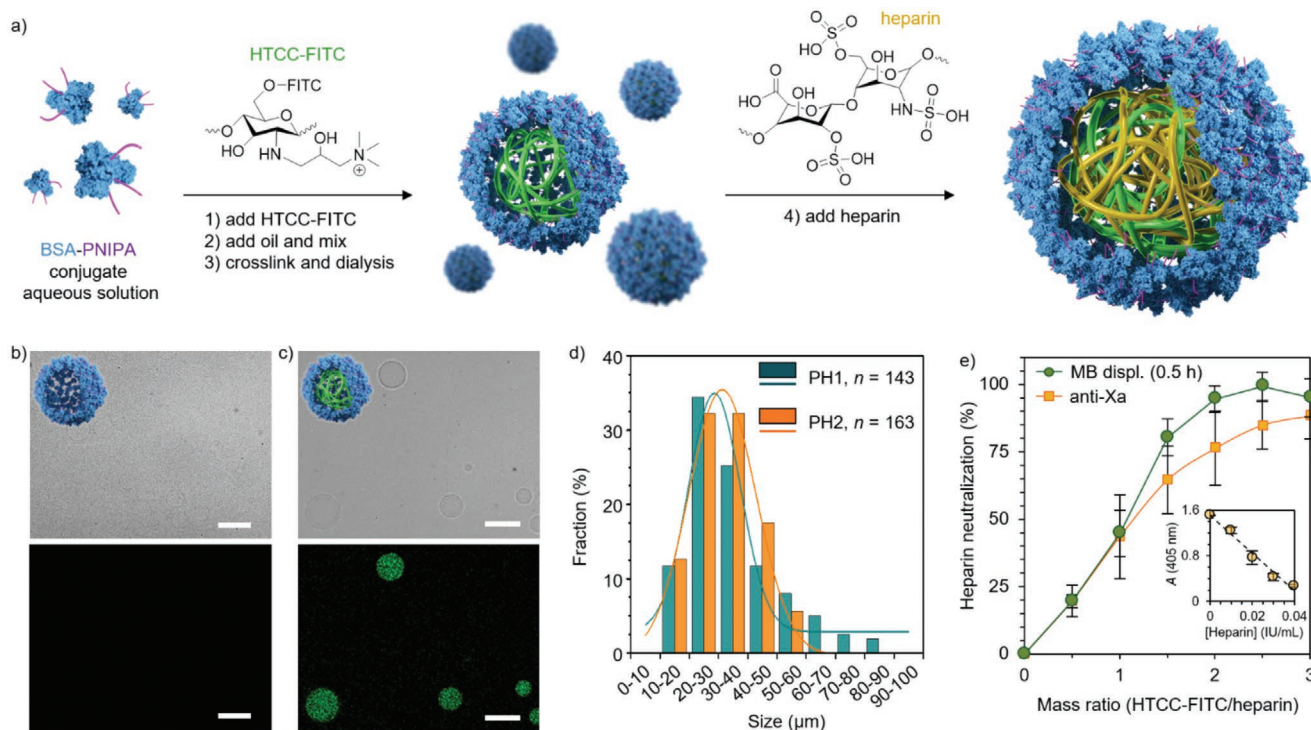
Figure 1. Preparation and characterization of HTCC-loaded proteinosomes. a) Schematic illustration of the preparation procedure and the subsequent application in heparin scavenging. CFM images of b) empty proteinosomes and c) those containing HTCC (local HTCC concentration: 0.23 mg mL⁻¹) under bright field and FITC channel. Scale bar: 50 μm. d) Size distribution of proteinosomes containing two local HTCC concentrations (PH1: 0.23 mg mL⁻¹; PH2: 0.77 mg mL⁻¹) derived from optical microscope images (total numbers: PH1: 143; PH2: 163). Solid curves show Gaussian fits. e) MB displacement assay and anti-Xa assay results of free HTCC at room temperature. Heparin concentration: 1.5 μg mL⁻¹ (0.3 IU mL⁻¹) in MB displacement assay and 0.04 IU mL⁻¹ in anti-Xa assay. Inset indicates the calibration curve of anti-Xa assay. Measurements were performed using triplicate samples, and the averaged results with standard deviation are presented. All experiments were performed at room temperature.

Information). The fluorescence intensities of FITC in HTCC-loaded proteinosomes were significantly higher compared to empty proteinosomes and remained the same after heparin internalization. In contrast, the HTCC-loaded proteinosomes showed enhanced Rhodamine B fluorescence after heparin-uptake, showcasing the successful encapsulation of HTCC and the electrostatically driven internalization of heparin.

The heparin-scavenging ability of proteinosomes under more physiologically relevant conditions (PBS) was evaluated with anti-Xa assay and flow cytometry (**Figure 2**a,b and Figure S11, Supporting Information). It was found that the presence of 150 M NaCl slowed down the heparin internalization into PH1: a saturation point was reached after 3 h (Figure 2a). This could be attributed to the screening effect of the high salt concentration.[19a] However, the change imposed on PH2 was small and a fast capture of heparin was observed (Figure 2b), which is driven by the higher cation charge density inside PH2 (Table S1, Supporting Information). A high optical contrast was also visualized after the anti-Xa assay within proteinosomes, demonstrating the formation of polyelectrolyte complexes (insets in Figure 2a,b). The flow cytometry analysis of PH1 (Figure S11, Supporting Information) and PH2 (Figure 2c,d) were similar to those at low salt conditions (Figure S10, Supporting Information). The broad distribution of FITC and Rhodamine B signals suggested the varied internal complexity of different protocells.

We also used CFM to visualize the real-time heparin-uptake process. Independent incubation of PH1 or PH2 with heparin under both conditions led to a distinguishable yellow fluorescence in proteinosomes, and the intensity was increased with incubation time, demonstrating the gradual uptake of heparin in proteinosomes (Figure 2e,f and Figures S12 and S13, Supporting Information). Distinct complex distribution patterns were observed within the two populations of proteinosomes: while the polyelectrolyte complexes in PH1 were distributed mainly along the interior surface, those in PH2 were homogeneously dispersed in the lumen, which may be attributed to the different local concentrations of HTCC (Figure 2e–g).[11] Solution electrolyte concentration can also play a role in determining the distribution patterns by screening the interaction between polyelectrolyte and protein membrane.[11] We also performed a control experiment showing that empty proteinosomes had a negligible uptake of heparin (Figure S14, Supporting Information). Upon incubation with proteinosomes, HSA (66.5 kDa) was also observed to traverse the membrane barrier (cutoff ca. 65 kDa) and complex with HTCC in both PH1 and PH2 under low-salt condition (Figure S15, Supporting Information). In the presence of 150 M NaCl, however, the interaction between HTCC and HSA was attenuated (Figure S16, Supporting Information), which could be attributed to the screening effect of high concentrations of salt.[19a]
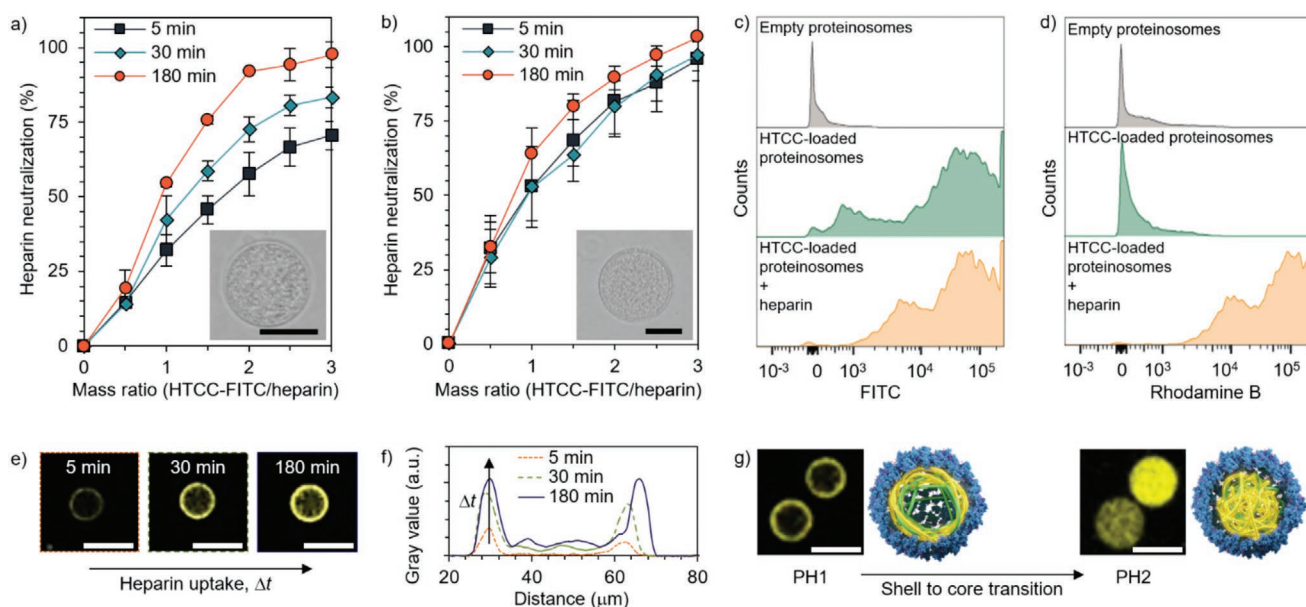
Figure 2. Evaluation on the heparin-scavenging ability of HTCC-loaded protocells. The time-dependent heparin-scavenging ability of a) PH1 and b) PH2 measured with anti-Xa assay in PBS. Measurements were performed using triplicate samples, and the averaged results with standard deviation are presented. Insets indicated the corresponding optical images of proteinosomes after the assay. Scale bar: 50 μm. FACS plots of FITC and Rhodamine B intensities in protocells (empty proteinosomes and PH2) showed the localization of c) FITC and d) Rhodamine B, demonstrating that heparin could only be captured by HTCC-containing proteinosomes in PBS. e) CFM images of PH1 incubated with heparin-Rhodamine B at different time points in PB. The increasing fluorescence intensity along the interior surface measured with CFM demonstrated the gradual uptake of heparin. Scale bar: 50 μm. f) Line profiles derived from CFM images of PH1 in e. g) The CFM images and the corresponding illustrative schemes showing the shell–to–core transition within proteinosomes as the local HTCC concentration was increased in PB. Scale bar: 50 μm. All experiments were performed at room temperature.

The heparin-scavenging performance of HTCC-loaded proteinosomes was then evaluated in the presence of HSA to simulate the competitive guest uptake in vivo. When the local HTCC concentration was low (PH1), only heparin was scavenged even at low salt concentration (Figure S17, Supporting Information), which contrasted with the behavior when incubated with HSA alone (Figure S15a, Supporting Information). Increasing salt concentration showed a negligible impact on the heparin-scavenging ability (Figure S18, Supporting Information). Increasing the local HTCC concentration inside proteinosomes (PH2) led to a synchronous fluorescence intensity increase of Rhodamine B and Cy5 in proteinosomes, indicating that both heparin and HSA were internalized simultaneously (**Figure 3**a). Considering the zeta potential measurements, it can be concluded that the low local HTCC concentration (PH1) showed a weak attractive force to guest molecules, and heparin was scavenged first because of the high charge density.[25] When the HTCC concentration was high (PH2), strong electrostatic interaction resulted in fast and simultaneous binding of heparin and HSA, leading to an unbiased guest molecule internalization as illustrated in Figure 3a. In the presence of 150 M NaCl, the binding between HTCC and guest molecules was slowed down, and selective heparin-scavenging was achieved due to its high anionic charge and multivalent electrostatic binding with HTCC (Figure 3b).[26] Therefore, together with the results obtained from the MB-displacement assay, it can be concluded that a selective internalization could be feasibly realized via adjusting local scavenger concentration and/or the environmental salt concentration.

After confirming the heparin-scavenging ability, we evaluated the biocompatibility of all heparin scavengers (HTCC, FITC-labeled HTCC, PH1, PH2 and PS) with hemolytic assay and 3-(4,5-dimethylthiazol-2-yl)-2,5-diphenyl-tetrazolium bromide (MTT) dye assay (**Figure 4**). Hemolytic assay revealed that all binders showed no detectable toxicity to red blood cells (RBCs) up to 100 μg mL⁻¹ (Figure 4a). When incubated with human dermal fibroblast (HDF) cells, HTCC and PS showed no obvious influence, but 100 μg mL⁻¹ FITC-labeled HTCC induced more than 50% cell death after 4 h (Figure 4b). After encapsulation into proteinosomes, the toxicity of FITC-labeled HTCC was largely reduced, and more than 75% of cells were alive even after incubation with 100 μg mL⁻¹ PH1, which could be attributed to the shielding effect of the compartment. The cells were also directly observed under the optical microscope after the MTT assay (Figure 4c–e and Figure S19, Supporting Information). Without proteinosomes, HDF cells covered most of the well and displayed a typical stretched morphology. After 4 h incubation with proteinosomes, the cell coverage and morphology were not affected with up to 10 μg mL⁻¹ proteinosomes, showing an excellent viability. Besides, spherical proteinosomes were also identified, demonstrating the integrity of proteinosomes in the cell-culture media.

3. Conclusion

In this work, we successfully utilized semipermeable proteinosomes to load a highly positively charged chitosan derivative,

ADVANCED
SCIENCE NEWS
www.advancedsciencenews.com

NANO · MICRO
small
www.small-journal.com
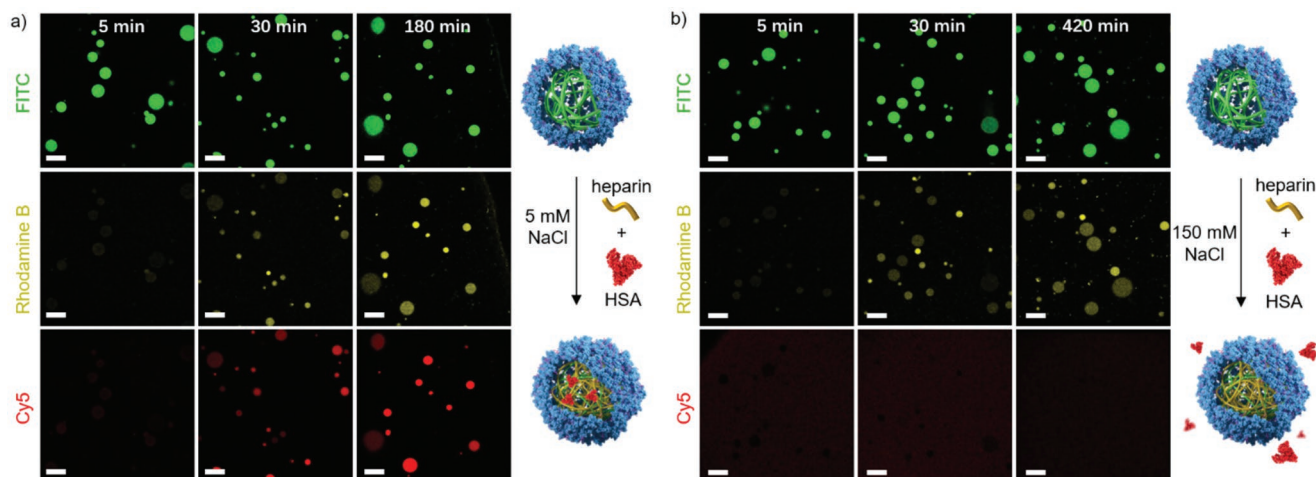
Figure 3. The time-dependent heparin-scavenging ability of PH2 in a) PB (5 M NaCl) and b) PBS (150 M NaCl) in the presence of HSA measured with CFM (Top row: FITC channel; middle row: Rhodamine B channel; bottom row: Cy5 channel). Scale bar: 100 µm. Images show that both heparin and HSA could enter PH2 at a low salt concentration (5 mM NaCl), but no HSA was scavenged under physiologically relevant conditions (150 mM NaCl) after longer incubation time, as depicted by the corresponding schematic presentation. All experiments were performed at room temperature.

HTCC, to reverse the anticoagulant agent, heparin. We found that free HTCC exhibited an excellent heparin-scavenging performance which was comparable to the clinically available antidote, PS. Owing to the highly cationic nature of HTCC and the semipermeable membrane of proteinosomes, the heparin-scavenging ability was largely retained after the encapsulation, and a time-dependent heparin-internalization was observed. We also demonstrated that a selective heparin-scavenging

ability over HSA could be realized via adjusting the local HTCC concentration or the surrounding salt concentration. Moreover, in vitro cell studies revealed excellent biocompatibility to RBCs and HDFs. Future studies should investigate for example the in vivo heparin-scavenging performance, immunocompatibility, and coagulation function. In summary, we believe that confined complexation presents a promising method for scavenging target polyelectrolytes, such as nucleic acids, in biologically
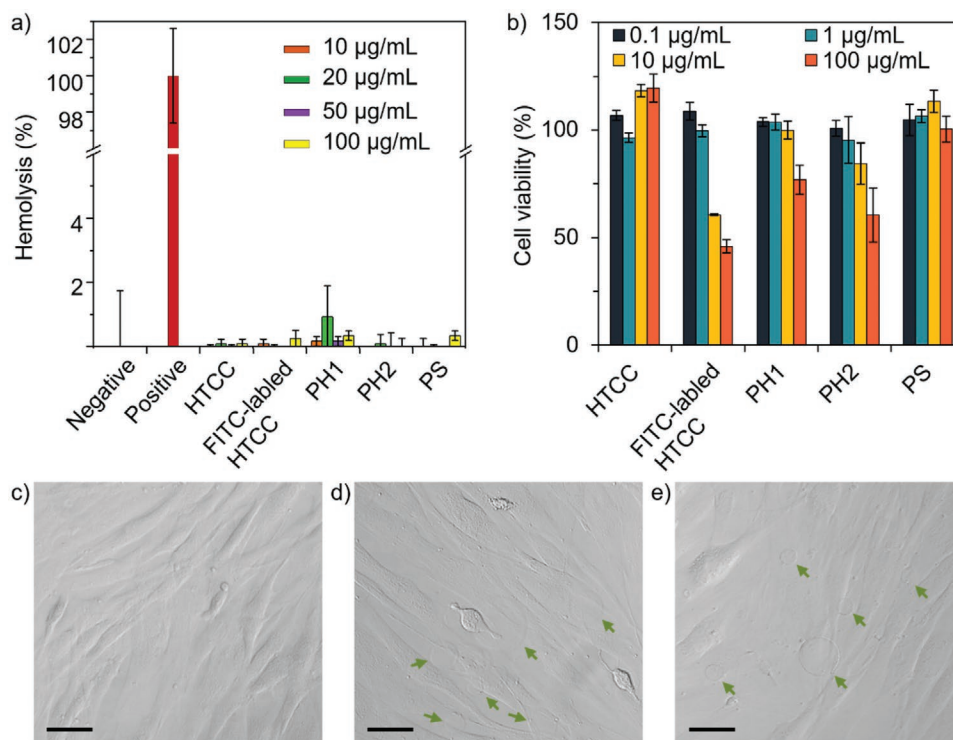
Figure 4. Biocompatibility evaluation of HTCC-loaded protocells measured with a) hemolysis assay and b) MTT assay. Measurements were performed using triplicate samples, and the averaged results with standard deviation are presented. Optical microscopy images of HDF cells after MTT assay incubated with c) PBS, d) PH1, and e) PH2. Final HTCC concentration: 1 µg mL⁻¹. Proteinosomes are indicated by green arrows in images. Scale bar: 50 µm.

ADVANCED
SCIENCE NEWS
www.advancedsciencenews.com

NANO · MICRO
small
www.small-journal.com

relevant conditions. Moreover, the clearance of other elements (e.g., heavy metal ions) can also be anticipated if appropriate scavengers are docked within the proteinosomes.

Conflict of Interest

The authors declare no conflict of interest.

Data Availability Statement

The data that support the findings of this study are available from the corresponding author upon reasonable request.

[1] L. C. Nelemans, L. Gurevich, *Materials* **2020**, *13*, 366.
[2] a) G. Sahay, D. Y. Alakhova, A. V. Kabanov, *J. Controlled Release* **2010**, *145*, 182; b) L. Y. T. Chou, K. Ming, W. C. W. Chan, *Chem. Soc. Rev.* **2011**, *40*, 233.
[3] J. A. Speir, S. Munshi, G. Wang, T. S. Baker, J. E. Johnson, *Structure* **1995**, *3*, 63.
[4] a) T. Douglas, M. Young, *Nature* **1998**, *393*, 152; b) Q. Liu, A. Shaukat, D. Kyllönen, M. A. Kostiainen, *Pharmaceutics* **2021**, *13*, 1551.
[5] J. E. Glasgow, M. A. Asensio, C. M. Jakobson, M. B. Francis, D. Tullman-Ercek, *ACS Synth. Biol.* **2015**, *4*, 1011.
[6] a) Y. Azuma, T. G. W. Edwardson, D. Hilvert, *Chem. Soc. Rev.* **2018**, *47*, 3543; b) T. G. W. Edwardson, S. Tetter, D. Hilvert, *Nat. Commun.* **2020**, *11*, 5410.
[7] a) M. Zhuang, Y. Zhang, S. Zhou, Y. Zhang, K. Wang, J. Nie, J. Liu, *Chem. Commun.* **2019**, *55*, 13880; b) D. Wang, S. Moreno, S. Boye, B. Voit, D. Appelhans, *Chem. Commun.* **2021**, *57*, 8019; c) Y. Elani, *Angew. Chem., Int. Ed.* **2021**, *60*, 5602.
[8] a) H. Che, S. Cao, J. C. M. Van Hest, *J. Am. Chem. Soc.* **2018**, *140*, 5356; b) Y. Ji, W. Mu, H. Wu, Y. Qiao, *Adv. Sci.* **2021**, *8*, 2101187; c) N. Gao, C. Xu, Z. Yin, M. Li, S. Mann, *J. Am. Chem. Soc.* **2022**, *144*, 3855.
[9] a) Y. Qiao, M. Li, R. Booth, S. Mann, *Nat. Chem.* **2017**, *9*, 110; b) H. Wu, X. Du, X. Meng, D. Qiu, Y. Qiao, *Nat. Commun.* **2021**, *12*, 6113; c) L. Rodríguez-Arco, B. V. V. S. P. Kumar, M. Li, A. J. Patil, S. Mann, *Angew. Chem., Int. Ed.* **2019**, *58*, 6333.
[10] a) X. Huang, M. Li, D. C. Green, D. S. Williams, A. J. Patil, S. Mann, *Nat. Commun.* **2013**, *4*, 2239; b) S. Yang, P. A. Pieters, A. Joesaar, B. W. A. Bögels, R. Brouwers, I. Myrgorodska, S. Mann, T. F. A. de Greef, *ACS Nano* **2020**, *14*, 15992; c) Y. Qiao, M. Li, D. Qiu, S. Mann, *Angew. Chem., Int. Ed.* **2019**, *58*, 17758.
[11] S. M. R. Booth, Y. Qiao, M. Li, *Angew. Chem., Int. Ed.* **2019**, *58*, 9120.
[12] W. Mu, Z. Ji, M. Zhou, J. Wu, Y. Lin, Y. Qiao, *Sci. Adv.* **2021**, *7*, eabf9000.
[13] a) S. Liu, Y. Zhang, M. Li, L. Xiong, Z. Zhang, X. Yang, X. He, K. Wang, J. Liu, S. Mann, *Nat. Chem.* **2020**, *12*, 1165; b) M. H. M. E. van Stevendaal, L. Vasiukas, N. A. Yewdall, A. F. Mason, J. C. M. van Hest, *ACS Appl. Mater. Interfaces* **2021**, *13*, 7879.
[14] a) S. M. Bromfield, E. Wilde, D. K. Smith, *Chem. Soc. Rev.* **2013**, *42*, 9184; b) E. I. Oduah, R. J. Linhardt, S. T. Sharfstein, *Pharmaceuticals* **2016**, *9*, 38.
[15] B. Girolami, A. Girolami, *Semin. Thromb. Hemostasis* **2006**, *32*, 803.
[16] E. Sokolowska, B. Kalaska, J. Miklosz, A. Mogielnicki, *Expert Opin. Drug Metab. Toxicol.* **2016**, *12*, 897.
[17] a) M. J. Hernaiz, L. A. LeBrun, Y. Wu, J. W. Sen, R. J. Linhardt, N. H. H. Heegaard, *Eur. J. Biochem.* **2002**, *269*, 2860; b) S. Välimäki, A. Khakalo, A. Ora, L. S. Johansson, O. J. Rojas, M. A. Kostiainen, *Biomacromolecules* **2016**, *17*, 2891; c) Q. Huang, H. Zhao, M. Shui, D.-S. Guo, R. Wang, *Chem. Sci.* **2021**, *11*, 9623.
[18] a) A. C. Rodrigo, A. Barnard, J. Cooper, D. K. Smith, *Angew. Chem., Int. Ed.* **2011**, *50*, 4675; b) L. E. Fechner, B. Albanyan, V. M. P. Vieira, E. Laurini, P. Posocco, S. Pricl, D. K. Smith, *Chem. Sci.* **2016**, *7*, 4653; c) V. M. P. Vieira, V. Liljeström, P. Posocco, E. Laurini, S. Pricl, M. A. Kostiainen, D. K. Smith, *J. Mater. Chem. B* **2017**, *5*, 341.
[19] a) Q. Liu, S. Välimäki, A. Shaukat, B. Shen, V. Linko, M. A. Kostiainen, *ACS Omega* **2019**, *4*, 21891; b) S. Välimäki, Q. Liu, L. Schoonen, D. F. M. Vervoort, Nonappa, V. L., R. J. M. Nolte, J. C. M. van Hest, M. A. Kostiainen, *J. Mater. Chem. B* **2021**, *9*, 1272.
[20] A. Joesaar, S. Yang, B. Bögels, A. van der Linden, P. Pieters, B. V. V. S. P. Kumar, N. Dalchau, A. Phillips, S. Mann, T. F. A. de Greef, *Nat. Nanotechnol.* **2019**, *14*, 369.
[21] S. H. Lim, S. M. Hudson, *Carbohydr. Res.* **2004**, *339*, 313.
[22] G. Fanali, A. D. Masi, V. Trezza, M. Marino, M. Fasano, P. Ascenzi, *Mol. Aspects Med.* **2012**, *33*, 209.
[23] a) K. Kaminski, K. Szczubiałka, K. Zazakowny, R. Lach, M. Nowakowska, *J. Med. Chem.* **2010**, *53*, 4141; b) B. Kalaska, K. Kaminski, E. Sokolowska, D. Czaplicki, M. Kujdowicz, K. Stalinska, J. Bereta, K. Szczubialka, D. Pawlak, M. Nowakowska, A. Mogielnicki, *PLoS One* **2015**, *10*, e0119486; c) B. Kalaska, J. Miklosz, K. Kaminski, J. Swieton, A. Jakimczuk, S.-I. Yusa, D. Pawlak, M. Nowakowska, K. Szczubiałka, A. Mogielnicki, *J. Pharmacol. Exp. Ther.* **2020**, *373*, 51.
[24] X. Huang, A. J. Patil, M. Li, S. Mann, *J. Am. Chem. Soc.* **2014**, *136*, 9225.
[25] a) S. Välimäki, N. K. Beyeh, V. Linko, R. H. A. Ras, M. A. Kostiainen, *Nanoscale* **2018**, *10*, 14022; b) Q. Liu, Z. Meng, A. Korpi, E. Kontturi, M. A. Kostiainen, *Chem. Eng. J.* **2021**, *420*, 129811.
[26] a) M. A. Kostiainen, J. G. Hardy, D. K. Smith, *Angew. Chem., Int. Ed.* **2005**, *44*, 2556; b) M. A. Kostiainen, G. R. Szilvay, J. Lehtinen, D. K. Smith, M. B. Linder, A. Urtti, O. Ikkala, *ACS Nano* **2007**, *1*, 103.